

UNCLASSIFIED

---

AD 257 396

*Reproduced  
by the*

ARMED SERVICES TECHNICAL INFORMATION AGENCY  
ARLINGTON HALL STATION  
ARLINGTON 12, VIRGINIA



---

UNCLASSIFIED

NOTICE: When government or other drawings, specifications or other data are used for any purpose other than in connection with a definitely related government procurement operation, the U. S. Government thereby incurs no responsibility, nor any obligation whatsoever; and the fact that the Government may have formulated, furnished, or in any way supplied the said drawings, specifications, or other data is not to be regarded by implication or otherwise as in any manner licensing the holder or any other person or corporation, or conveying any rights or permission to manufacture, use or sell any patented invention that may in any way be related thereto.

227100

257 396

AFOSR 622

# CORNELL AERONAUTICAL LABORATORY, INC.

CATALOGED BY ASTIA  
AS AD NO

XEROX

REPORT NO. AF-1413-A-1  
 EXACT SOLUTIONS FOR NONEQUILIBRIUM EXPANSIONS  
 OF AIR WITH COUPLED CHEMICAL REACTIONS  
 by  
 Alan Q. Eschenroeder, Donald W. Boyer  
 and  
 J. Gordon Hall  
 MAY 1961  
 Contract No. AF 49(638)-792

ASTIA  
 JUN 12 1961  
 TIFDR. A

#260

B U F F A L O , N E W Y O R K

AFOSR 622



CORNELL AERONAUTICAL LABORATORY, INC.  
Buffalo 21, New York

REPORT NO. AF-1413-A-1

EXACT SOLUTIONS FOR NONEQUILIBRIUM EXPANSIONS  
OF AIR WITH COUPLED CHEMICAL REACTIONS

MAY 1961

Contract No. AF 49(638)-792

Mechanics Division  
Air Force Office of Scientific Research  
Air Research and Development Command  
Washington, D.C.

BY: Alan Q. Eschenroeder  
Alan Q. Eschenroeder

APPROVED: A. Hertzberg  
A. Hertzberg, Head  
Aerodynamic Research Department

Donald W. Boyer  
Donald W. Boyer

J. Gordon Hall  
J. Gordon Hall

## ABSTRACT

Results of numerical integrations of the coupled chemical rate equations and gasdynamic equations are presented for nozzle airflows over a wide range of conditions appropriate to high performance hypersonic tunnel testing<sup>1</sup>. Composition histories are shown for a kinetic mechanism including six species and fourteen reactions. Gasdynamic effects of nonequilibrium processes qualitatively resemble those reported earlier<sup>2</sup>. However, the freezing process is more complex because the nitric-oxide shuffle reactions couple the dissociation-recombination reactions. In many cases where the energy in nitrogen dissociation is significant, the fast shuffle reactions prevent nitrogen atom freezing which would otherwise occur if three-body recombination were the only process operating. Nitric oxide concentrations undershoot the equilibrium values in many cases. Oxygen freezing is affected little by the shuffle reactions. The detailed results suggest the applicability of simplified chemical kinetic models based on the shuffle reactions for airflows in various regimes of the initial state. The range of validity of a previous model<sup>2</sup> based on oxygen dissociation-recombination in air is also indicated by the results.

## FOREWORD

The airflow computations reported herein and the preparation of this report were sponsored by the Mechanics Branch of the Air Force Office of Scientific Research under Contract AF 49(638)-792. The computations were carried out with IBM 704 machine programs developed for computation of equilibrium and nonequilibrium flows of multicomponent reacting systems. Analytic formulation of the general reacting flow problem was done under Air Force Contract AF 40(600)-804. This contract also supported subsequent coding and development of the equilibrium flow program. Coding and development of the nonequilibrium flow program was supported by Cornell Aeronautical Laboratory Internal Research.

Grateful acknowledgement of assistance is made to Dr. John Fleck, Head, Computer Systems Branch, Systems Research Department, without whose efforts the successful development of the machine programs would not have been possible.

## LIST OF SYMBOLS

$a$	-	Tangent of semi-angle included by the asymptotic cone of the nozzle
$A$	-	Local to throat area ratio
$H$	-	Enthalpy
$k$	-	Rate constant
$\ell$	-	Nozzle scale parameter
$L$	-	Nozzle throat radius
$M$	-	Mach number
$P$	-	Pressure
$Re$	-	Reynolds number
$T$	-	Absolute temperature
$U$	-	Velocity
$x'$	-	Axial distance downstream from throat
$\theta_D$	-	Characteristic temperature of dissociation
$\rho$	-	Density

### Subscripts

$EQ$	-	Equilibrium conditions
$f$	-	Forward reaction
$F$	-	Frozen conditions
$o$	-	Initial conditions

## INTRODUCTION

Many studies of chemical nonequilibrium effects on high-enthalpy expanding flows have been reported previously<sup>2-8</sup>. Vincenti has reviewed this work comprehensively in a recent report<sup>9</sup>. The need for performance predictions for rocket and hypersonic wind-tunnel nozzles has lent impetus to such studies. Moreover, investigation of expanding flows about bodies moving at high speeds and altitudes is another area of similar nonequilibrium problems. The great majority of these flows involve gaseous mixtures undergoing many interdependent chemical reactions which interact with the gasdynamic processes.

Much of the previous work treats binary mixtures only; however, in some studies, simplified models based on a single nonequilibrium process have been employed under the assumption that one reaction controls the overall thermodynamic or rate behavior of multicomponent mixtures. One of the earliest treatments was developed by Penner<sup>4</sup> for a reactive mixture expanding in a rocket nozzle. His method, based on linear criteria for near-equilibrium and near-frozen flow, was subsequently applied to the hydrogen-fluorine system<sup>5</sup>. The disappearance of carbon monoxide was assumed by Reynolds and Baldwin<sup>6</sup> and the decomposition of the hydroxyl radical was assumed by Browne<sup>7</sup> as the dominant process in hydrocarbon-air combustion products flowing through a nozzle. The use of a simple model for airflows was developed by Hall and Russo<sup>2</sup> and was extended and applied to a wide range of flow conditions by Boyer, Eschenroeder, and Russo<sup>8</sup>. This model for air allows oxygen dissociation-recombination processes to depart from equilibrium while all other reactions are either frozen or remain equilibrated.

Recently, concentrated efforts devoted to the study of air kinetics have yielded a body of information on the significant elementary processes (e.g. Refs. 10-14.) Although the accuracy of these experimental data may be further improved, it is now worthwhile to develop methods for solving exactly the coupled equations of chemistry and fluid mechanics for multiple reactions.

An IBM 704 computing machine program\* has been developed at Cornell Aeronautical Laboratory for solving the equilibrium and nonequilibrium flows of arbitrarily complex reactive mixtures in quasi-one-dimensional expansions. The analytical approach will be presented in a later report. Although the present application of the method has been limited to finite-rate chemical problems, the machine code has been written to include ionization nonequilibrium effects and vibrational nonequilibrium coupling with the caloric and chemical behavior of the gas.

The present note contains the results of calculations for the expansion of air undergoing multiple coupled chemical reactions in a hypersonic nozzle. The chemical mechanism includes dissociation-recombination reactions of  $O_2$ ,  $N_2$ , and NO and the bimolecular NO exchange reactions. A significant role is played by the nitric oxide shuffle reactions in delaying N-atom freezing and causing NO-undershoot. Oxygen freezing, however, is influenced only slightly by the shuffle reactions. The composition histories will be discussed in detail and the gas-dynamic effects in the hypersonic flow will be briefly summarized, following a listing of the assumptions utilized in the analytical formulation.

---

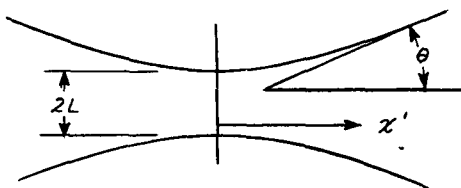
\* The Fortran computer program was written and coded by John Fleck, Leonard Garr, and Duane Larson of the Systems Research Department of Cornell Aero. Lab, Inc.

## ASSUMPTIONS IN THE ANALYSIS

A quasi-one-dimensional flow of an ideal gas mixture was assumed to occur under steady adiabatic conditions free of transport effects. In particular, critical nozzle flows were calculated for an air model composed of the monatomic species, N, O, Ar, and the diatomic species O<sub>2</sub>, N<sub>2</sub>, and NO. The caloric model for diatomic species included equilibrium vibrational excitation according to a linear oscillator model in addition to equilibrium translational, rotational, and electronic contributions.

For the initial departures from chemical equilibrium, linearized perturbation techniques with their attendant assumptions were adopted. An axisymmetric hyperbolic nozzle geometry following the law  $A = 1 + \left(\frac{x'}{\ell}\right)^2$  was used in the present calculations. As illustrated in the sketch below, A is the local to throat area ratio, x' is the axial distance downstream from the throat, and  $\ell$  is the ratio of throat radius L to the tangent  $\alpha$  of the semi-angle of the asymptote cone. Calculations were done for  $\ell = 1$  cm. as this value typifies many hypersonic shock tunnel nozzles.

$$A = 1 + \left(\frac{x'}{\ell}\right)^2$$



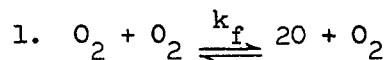
$$\ell = \frac{L}{\tan \theta}$$

Axisymmetric Hyperbolic Nozzle Geometry

The chemical composition of the air (O<sub>2</sub>, N<sub>2</sub>, Ar, O, N, NO) undergoing expansion was assumed to be governed by the three-body dissociation-recombination kinetics of oxygen, nitrogen, and nitric oxide (reactions 1 to 12 below) and by the two nitric oxide "shuffle" reactions (reactions 13 and 14 below.) The

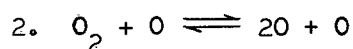
relative effectiveness of the significant second and third bodies was considered for the  $O_2$  and  $N_2$  dissociation reactions. The ratio of forward to reverse reaction rate constants was taken to be the equilibrium constant.

The elementary reactions and pertinent rate data employed were as follows:



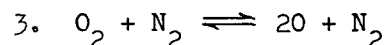
Byron's<sup>9</sup> value was used for the dissociation rate constant.

$$k_{f_1} = 3.56 \times 10^{21} T^{-3/2} \exp\left(-\frac{59380}{T}\right) \text{ cm}^3/\text{mole sec.}$$



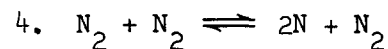
The steric factors for the  $O_2$  dissociation reaction, obtained from fits to experimental data<sup>10</sup>, indicate the effectiveness of the O atom as a third body to be  $35 \frac{T}{\theta_D}$  times that of the  $O_2$  molecule, where  $\theta_D$  is the characteristic dissociation temperature for oxygen (59400°K). This relative efficiency for O is slightly less than the factor of 5 generally assumed<sup>11</sup>.

$$k_{f_2} = 35 \frac{T}{\theta_D} k_{f_1} = 2.1 \times 10^{18} T^{-1/2} \exp\left(-\frac{59380}{T}\right) \text{ cm}^3/\text{mole sec.}$$



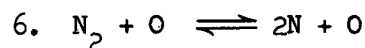
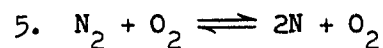
The rate constant for this reaction has not been directly measured but the effectiveness of the  $N_2$  molecule is generally assumed to be 1/3 that of the  $O_2$  molecule<sup>11</sup>.

$$k_{f_3} = 1.19 \times 10^{21} T^{-3/2} \exp\left(-\frac{59380}{T}\right) \text{ cm}^3/\text{mole sec.}$$



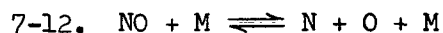
The recombination rate constants reported by Wray et al<sup>11</sup> and Hammerling et al<sup>12</sup> were used and the corresponding dissociation rates calculated from the recombination rate and the equilibrium constant

$$k_{f_4} = 29.7 \times 10^{20} T^{-3/2} \exp\left(-\frac{113260}{T}\right) \text{ cm}^3/\text{mole sec.}$$



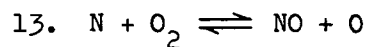
The oxygen atom and molecule were assumed equally effective but of only 1/3 the catalytic efficiency of the  $\text{N}_2$  molecule<sup>11</sup>.

$$k_{f_{5,6}} = 9.2 \times 10^{20} T^{-3/2} \exp\left(-\frac{113260}{T}\right) \text{ cm}^3/\text{mole sec.}$$



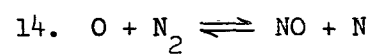
The NO dissociation reaction was considered for a general third body, i.e. catalyst M may be any of the 6 species available, all being considered of equal effectiveness. It is generally assumed that the argon atom as a third body has only about 1/6 the efficiency of any other particle present<sup>11</sup>. However, the effective increase in the argon atom efficiency by this lumped third body dependence will have a small effect because of the low argon concentration. There is, in fact, experimental evidence<sup>13</sup> to support such an increase in the argon efficiency. The forward rate constant was obtained from the recombination rate given in Ref. 11 and the equilibrium constant. For all third bodies

$$k_{f_{7-12}} = 5.18 \times 10^{21} T^{-3/2} \exp\left(-\frac{75490}{T}\right) \text{ cm}^3/\text{mole sec.}$$



The reaction rate is somewhat uncertain and is based on extrapolated low temperature data, adjusted according to the experimental evidence of Wray and Teare<sup>13</sup>. The activation energy of the reverse reaction is large compared with that of the forward rate given here. The following value for the forward rate constant was used.<sup>11</sup>

$$k_{f_{13}} = 1 \times 10^{12} T^{1/2} \exp\left(-\frac{3120}{T}\right) \text{ cm}^3/\text{mole sec.}$$



The activation energy for the reverse rate of this reaction is comparatively small. The rate constant used for the forward reaction was that determined experimentally by Glick et al<sup>14</sup>:

$$k_{f_{14}} = 50 \times 10^{12} \exp\left(-\frac{38016}{T}\right) \text{ cm}^3/\text{mole sec.}$$

## DISCUSSION OF RESULTS

### Chemical Behavior

The composition histories of atomic species differ markedly from those which would be predicted by a binary gas model in the high-temperature range. Owing to the coupling through the bimolecular shuffle reactions (13) and (14), the freezing of nitrogen atoms is not nearly as rapid as that of oxygen atoms. If three-body recombinations were occurring alone, the opposite would occur because of the high activation energy of nitrogen dissociation. The bimolecular reaction paths which consume N-atoms have relatively low activation energies; therefore, even at modest concentrations of  $O_2$  or NO, they are far more efficient than three-body recombination in delaying N-atom freezing. Reactions (13) and (14) do not delay oxygen atom freezing because those consuming O have substantially higher activation energies, thereby introducing a strong temperature dependence in the decay of their rates during the expansion process. Thus, reactions (13) and (14) not only fail to provide fast paths for O-atom removal, but they produce more O-atoms after the three-body oxygen recombination has frozen.

Figure 1, showing air composition plotted against area ratio for stagnation conditions of  $T_o = 8000^{\circ}K$  and  $p_o = 100$  atm., strikingly illustrates the role of the shuffle reactions. In order to remove the effect of fluid density variation in the expansion, mass concentrations in moles per gram of mixture are used leaving only the influence of chemical reactions. Since the dissociation energy of nitrogen is nearly twice that of oxygen, the energetic contribution of N-atoms approximately equals that of O-atoms at the stagnation state chosen for Fig. 1. Freezing of oxygen atoms takes place nearly at the nozzle throat. At an area ratio of about 1.5, nitric oxide begins falling below its equilibrium concentration, and nitrogen atoms exhibit small upward departures from equilibrium.

It is important to note that the nitrogen atom concentration follows closely the steeply descending equilibrium curve over a considerable portion of the expansion. When nitrogen finally freezes, the level of dissociation is only about one-percent of the reservoir value. In contrast, oxygen freezing occurs at nearly the reservoir concentration.

The nitric oxide concentration exhibits an undershoot below the equilibrium curve. Reactions (13) and (14) compete for production and consumption of NO respectively. Consumption dominates because the N-NO collision rate is considerably higher than the N-O<sub>2</sub> rate. Since both reactions have weak temperature dependence in the directions considered, the collision rates principally determine the reaction rates. After all reactions freeze, the descending equilibrium curve for NO eventually intersects the nonequilibrium curve terminating the undershoot.

The influence of stagnation pressure on the reaction system may be seen by comparing Figs. 1, 2, 3, and 4. For  $p_0 = 10$ -atm. as shown in Fig. 2, O is frozen at the throat and N descends only a few percent before freezing. Clearly at low enough collision rates, even the two-body reactions cannot maintain equilibrium. A very large NO-undershoot is observed because the NO-concentration is at a considerably higher level than the O<sub>2</sub>-concentration. Figure 3 shows a moderate amount of N-atom decrease before freezing for  $p_0 = 30$  atm. It is interesting to note here that as NO and O<sub>2</sub> decay rapidly, the N-atom freezing occurs because the two molecular species are not available in sufficient quantity to maintain fast rates in the fast shuffle reactions. As shown in Fig. 4, the N-atoms are nearly equilibrated throughout the expansion from  $p_0 = 1000$  atm. The NO undershoot vanishes because the ratio of O<sub>2</sub> to NO concentration is unity or higher during oxygen atom freezing.

Comparison of Figs. 5, 6, and 7 with the plots for  $T_0 = 8000^\circ\text{K}$  shows the effect of temperature level. At the lower stagnation temperatures, the initial level of N-atom concentration is so small that its energetic contribution to the

gasdynamic properties is negligible. Nevertheless, it is instructive to observe that nitrogen equilibration is essentially complete. Figure 5 for  $T_0 = 6000^\circ\text{K}$ ,  $p_0 = 100$  atm. shows a slight NO-undershoot because oxygen freezes prior to the area ratio at which the  $\text{O}_2$ -concentration equals the NO-concentration. In general, oxygen nonequilibrium effects occur earlier at low stagnation temperatures because the equilibrium curves for O-atoms descend more rapidly than at the high temperatures. Because the shuffle reactions are not efficient in removing oxygen atoms, previous results<sup>2,8</sup> based on a single dissociation-recombination model for oxygen in air agree well with the exact solutions in the range  $T_0 \leq 6000^\circ\text{K}$ .

#### Gasdynamic Effects

Following the above considerations of the chemical composition effects, the influences of nonequilibrium on the gasdynamic variables in the nozzle flow may be briefly examined. As is well known, chemical freezing withholds energy from the active modes causing the static temperature to drop below the equilibrium value. Static pressures are also lowered by nonequilibrium phenomena. Previous studies have shown that if a substantial fraction of the total enthalpy is frozen, the effects on temperature and pressure can be very large. In contrast, the fluid density and velocity are only slightly affected. The net effect of these departures is an increase in the flow Mach number at a given station along the nozzle.

Table I summarizes the gasdynamic effects of chemical nonequilibrium for hypersonic expansions from reservoir states of 6000 and 8000 $^\circ\text{K}$  at 100 and 1000 atm. pressure. With the exception of the enthalpy H, ratios of the actual to equilibrium value of each variable are shown for expansions giving equilibrium airflow Mach numbers of 20. The first line in the tabulation is the frozen enthalpy divided by the total enthalpy of the flow. Mach number is defined here

as  $u / \left( \frac{dp}{dx} / \frac{d\rho}{dx} \right)^{1/2}$ , where  $u$  is the velocity,  $\rho$  is density, and  $p$  is pressure. The ratios of Reynolds numbers were calculated assuming a linear viscosity-temperature law.

The table illustrates the strong dependence of nonequilibrium effects on the initial state of the gas. The range of stagnation conditions considered is appropriate to hypersonic shock tunnel operation at high temperatures. In all cases shown, the frozen enthalpy consists almost entirely of the frozen energy of dissociation of oxygen; nitrogen freezing is energetically unimportant. At 8000°K and 100 atm., the dissociation energy of nitrogen constitutes about 25% of the stagnation enthalpy. However, this energy is completely recovered in the nozzle expansion because of the fast nitric-oxide shuffle reactions, as previously discussed. The importance of operating at high pressures in order to minimize nonequilibrium gasdynamic effects will be noted. At 1000 atm. stagnation pressure, nonequilibrium effects are greatly reduced compared with those at 100 atm. At 6000°K stagnation temperature, Table I indicates that operation at 1000 atm. suppresses nonequilibrium to an acceptable level for many shock tunnel studies.

## CONCLUSIONS

In addition to verifying trends predicted by previous work<sup>2,8</sup>, the results presented here reveal new information about the detailed chemical behavior of high-enthalpy air expansions. Over a considerable range of hypersonic tunnel conditions where nitrogen dissociation contributes significantly to the total energy, the freezing of nitrogen atoms is sufficiently delayed by the fast nitric oxide shuffle reactions so that it may be neglected in gasdynamic calculations. The stored energy in this mode, therefore, is essentially completely recovered as flow kinetic energy unless the stagnation pressures are rather low. If the  $O_2$ -concentration is below the NO-concentration during oxygen atom freezing, an NO-undershoot occurs over a large part of the expansion. O-atom freezing is little affected by the nitric oxide shuffle reactions.

Considerable simplification of the air kinetic model is possible in certain regimes. At pressures low enough to cause early freezing of N and O, NO and  $O_2$  could be used as composition variables with the reaction  $N + NO \rightleftharpoons N_2 + O$ . This is a good approximation of the complete kinetics because the ratio of  $O_2$ -concentration to NO-concentration is small. The temperature-density history of a frozen flow would be employed in such a model since the reaction given has little influence on the gasdynamics. At high pressures, the freezing of the oxygen dissociation-recombination process could be considered to be the only nonequilibrium reaction in the early stages of the expansion. Subsequent to this, the  $N + NO$  reaction would control the N-atom freezing in cases where the  $O_2$ -concentration is much smaller than the NO-concentration. Therefore, the approximate model for air previously employed<sup>8</sup> for temperatures up to  $6000^\circ K$  can probably be extended to higher temperatures involving significant energy in nitrogen dissociation. Such extension may be made provided the pressure is high

enough for reaction [14 (reverse)] to remove most of the N-atoms. At conditions yielding initial  $O_2$ -concentrations comparable with NO-concentrations, the energy represented by nitrogen dissociation is small and the question of nitrogen equilibration becomes unimportant.

## REFERENCES

1. Hertzberg, A. and Wittliff, C. E., Studying Hypersonic Flight in the Shock Tunnel. IAS Paper No. 60-67 (June 1960).
2. Hall, J. G. and Russo, A. L., Studies of Chemical Nonequilibrium in Hypersonic Nozzle Flows. Cornell Aeronautical Laboratory Report No. AD-1118-A-6, (AFOSR TN 59-1090), (November 1959). Also in the Proceeding of the First Conference on Kinetics, Equilibria and Performance of High Temperature Systems, Butterworths, London (1960).
3. Bray, K. N. C., Departure from Dissociation Equilibrium in a Hypersonic Nozzle. Aeronautical Research Report 19, 938 (March 1958).
4. Penner, S. S., J. Chem. Phys. 17 (1949) 841.
5. Penner, S. S., J. Franklin Inst. 249 (1950) 441.
6. Reynolds, T. W. and Baldwin, L. V., One Dimensional Flow with Chemical Reaction in Nozzle Expansions. Paper at the Symposium on Thermodynamics of Jet and Rocket Propulsion, A. I. Ch. E., (May 1959).
7. Browne, W. G., The Recombination Problem in a Jet Exhaust Nozzle. Paper 59-105 at the Summer Meeting IAS, (June 1959).
8. Boyer, D. W., Eschenroeder, A. Q., and Russo, A. L., Approximate Solutions for Nonequilibrium Airflow in Hypersonic Nozzles. Cornell Aeronautical Laboratory Report No. AD-1345-W-3 (AEDC TN 60-181), (August 1960).
9. Vincenti, W. G., Calculations of the One-Dimensional Nonequilibrium Flow of Air Through a Hypersonic Nozzle - Interim Report. Stanford University, Department of Aero. Engineering Report No. 101, (January 1961).
10. Byron, S. B., Interferometric Measurement of the Rate of Dissociation of Oxygen Heated by Strong Shock Waves. Cornell University Report (1958).
11. Wray, J. D., Teare, J. D., Kivel, B., and Hammerling, P., Relaxation Processes and Reaction Rates Behind Shock Fronts in Air and Component Gases. AVCO Research Report No. 83, (December 1959).
12. Hammerling, P., Teare, J. D., and Kivel, B., Theory of Radiation from Luminous Shock Waves in Nitrogen. AVCO Research Report No. 49, (June 1959).
13. Wray, K. L. and Teare, J. D., Kinetic Studies of Nitric Oxide. AVCO Research Note No. 134, (June 1959).
14. Glick, H. S., Klein, J. J., and Squire, W. J., J. Chem. Phys. 27 (1957) 850.

TABLE I - RATIOS OF ACTUAL TO EQUILIBRIUM AIRFLOW VARIABLES FOR  
COUPLED-REACTION EXPANSIONS GIVING EQUILIBRIUM MACH NUMBER 20

$L/a = 1 \text{ cm.}$

$T_o$	6000°K		8000°K	
$P_o$	100 atm.	1000 atm.	100 atm.	1000 atm.
$H_F/H_O$	.155	.048	.194	.0813
$P/P_{EQ}$	0.425	0.875	0.159	0.544
$T/T_{EQ}$	0.359	0.855	0.121	0.497
$\rho/\rho_{EQ}$	1.095	1.014	1.110	1.045
$u/u_{EQ}$	0.913	0.987	0.901	0.957
$M/M_{EQ}$	1.455	1.06	2.30	1.305
$Re_x/Re_{x_{EQ}}$	2.79	1.17	8.25	2.01

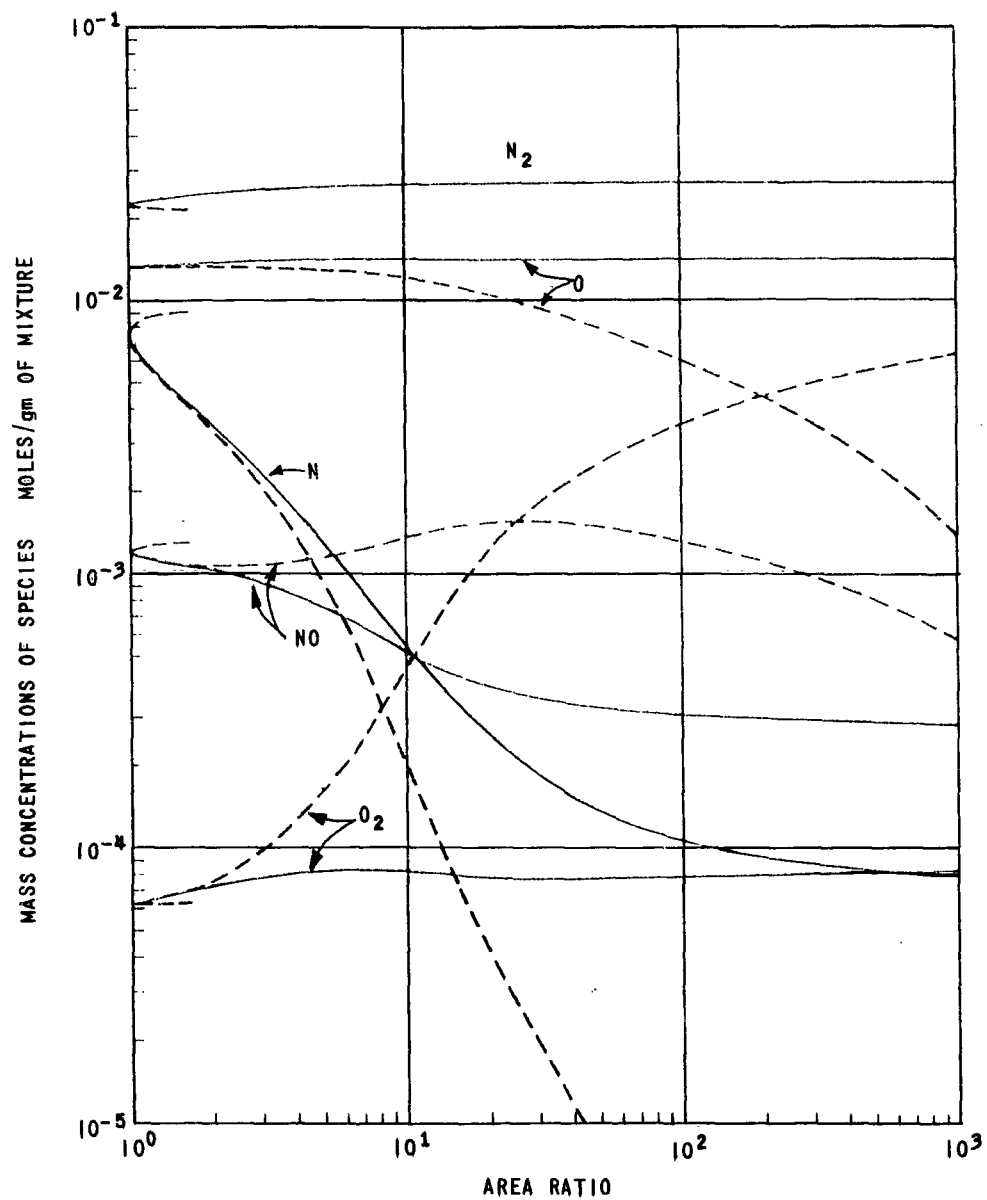


FIG. 1 SPECIES DISTRIBUTIONS FOR AIRFLOW IN A HYPERSONIC NOZZLE

$$T_0 = 8000^\circ\text{K}, P_0 = 100 \text{ ATM } l = 1 \text{ cm}$$

———— FINITE RATE NONEQUILIBRIUM  
 - - - - - INFINITE RATE EQUILIBRIUM

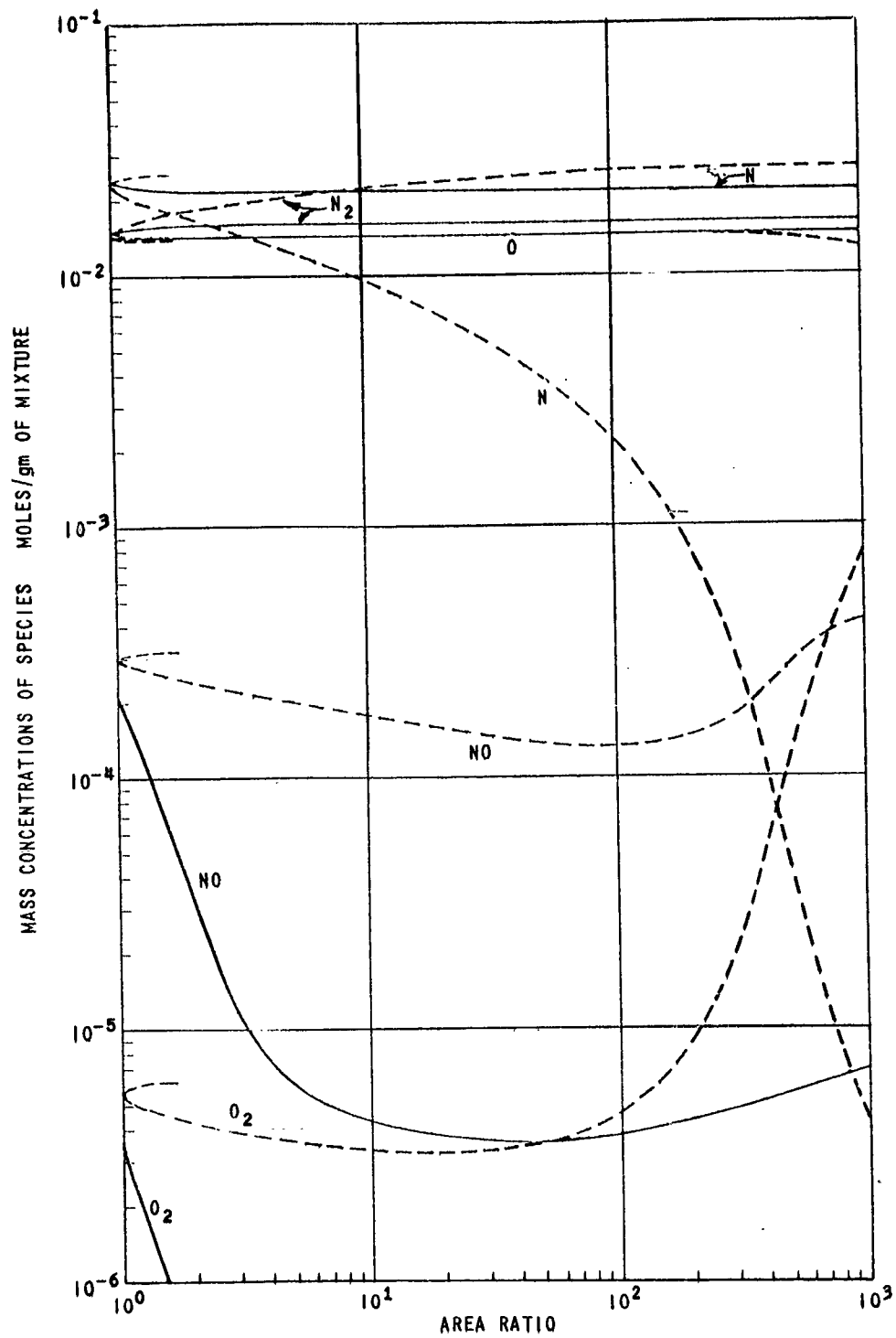


FIG. 2 SPECIES DISTRIBUTIONS FOR AIRFLOW IN A HYPERSONIC NOZZLE

$$T_0 = 8000^\circ K, P_0 = 10 \text{ ATM } \ell = 1 \text{ cm}$$

— FINITE RATE NONEQUILIBRIUM

- - - INFINITE RATE EQUILIBRIUM

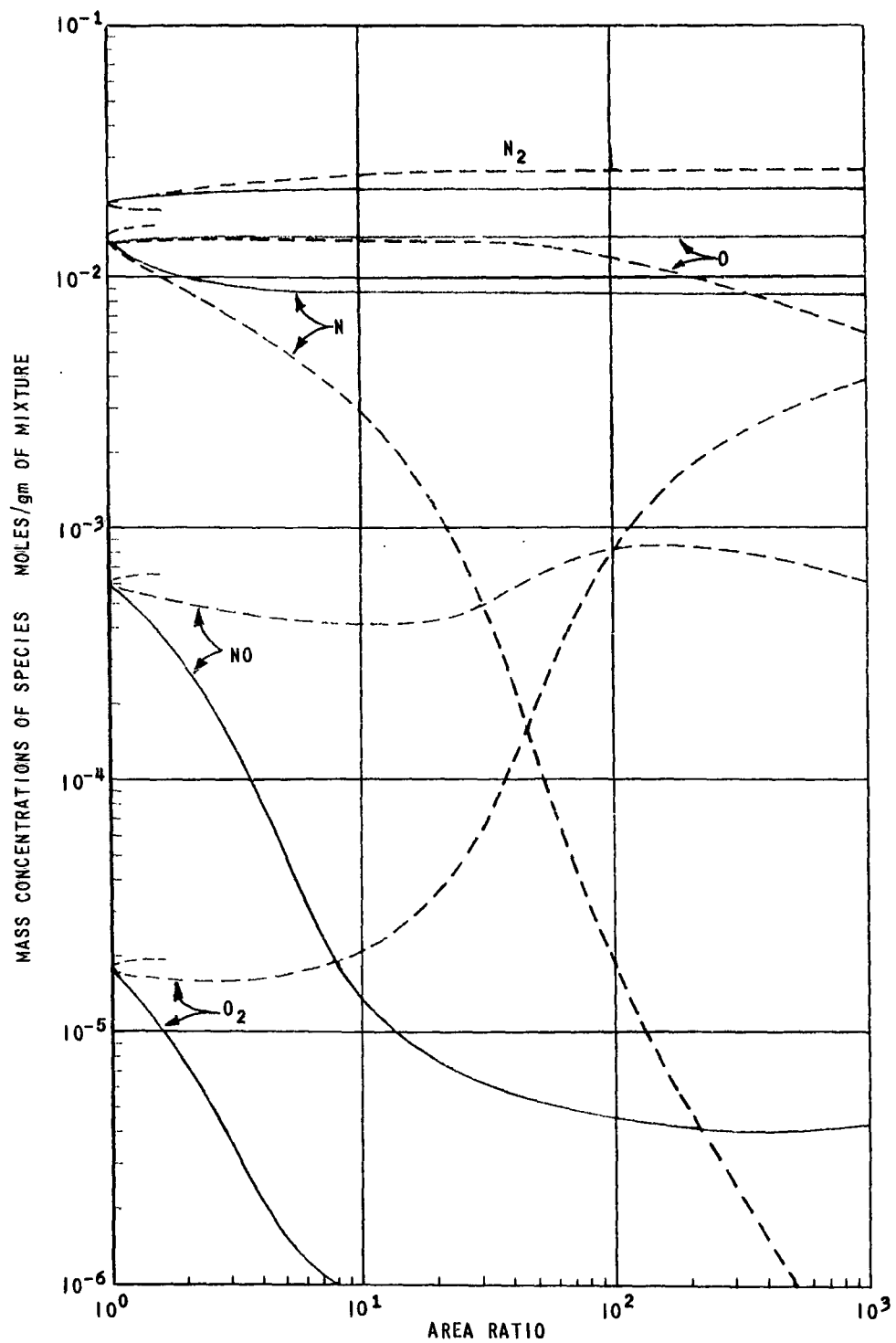


FIG. 3 SPECIES DISTRIBUTIONS FOR AIRFLOW IN A HYPERSONIC NOZZLE

$$T_0 = 8000^\circ K \quad P_0 = 30 \text{ ATM} \quad L = 1 \text{ cm}$$

———— FINITE RATE NONEQUILIBRIUM  
 - - - - - INFINITE RATE EQUILIBRIUM

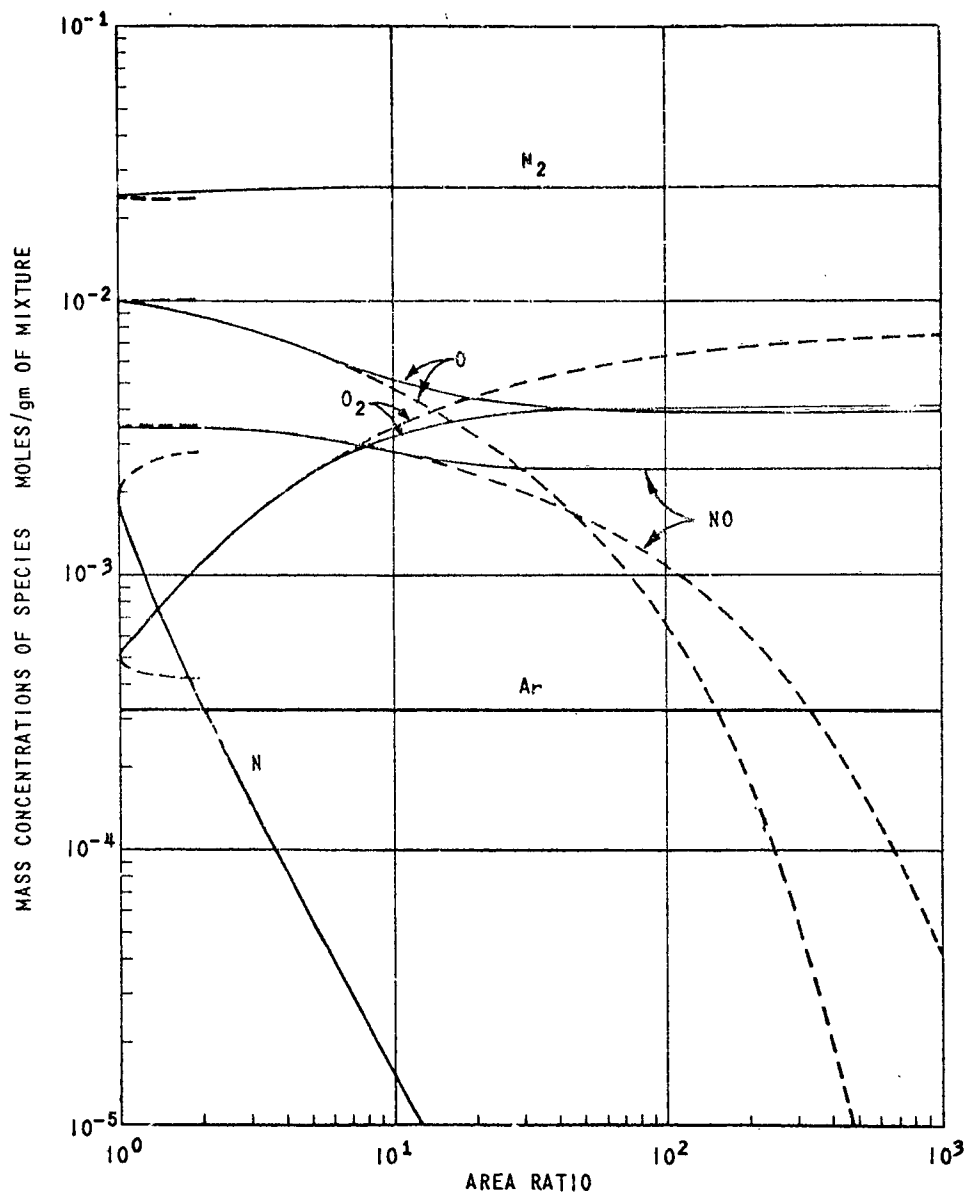


FIG. 4 SPECIES DISTRIBUTIONS FOR AIRFLOW IN A HYPERSONIC NOZZLE

$$T_0 = 8000^\circ K, \rho_0 = 1000 \text{ ATM } l = 1 \text{ cm}$$

———— FINITE RATE NONEQUILIBRIUM  
 - - - INFINITE RATE EQUILIBRIUM

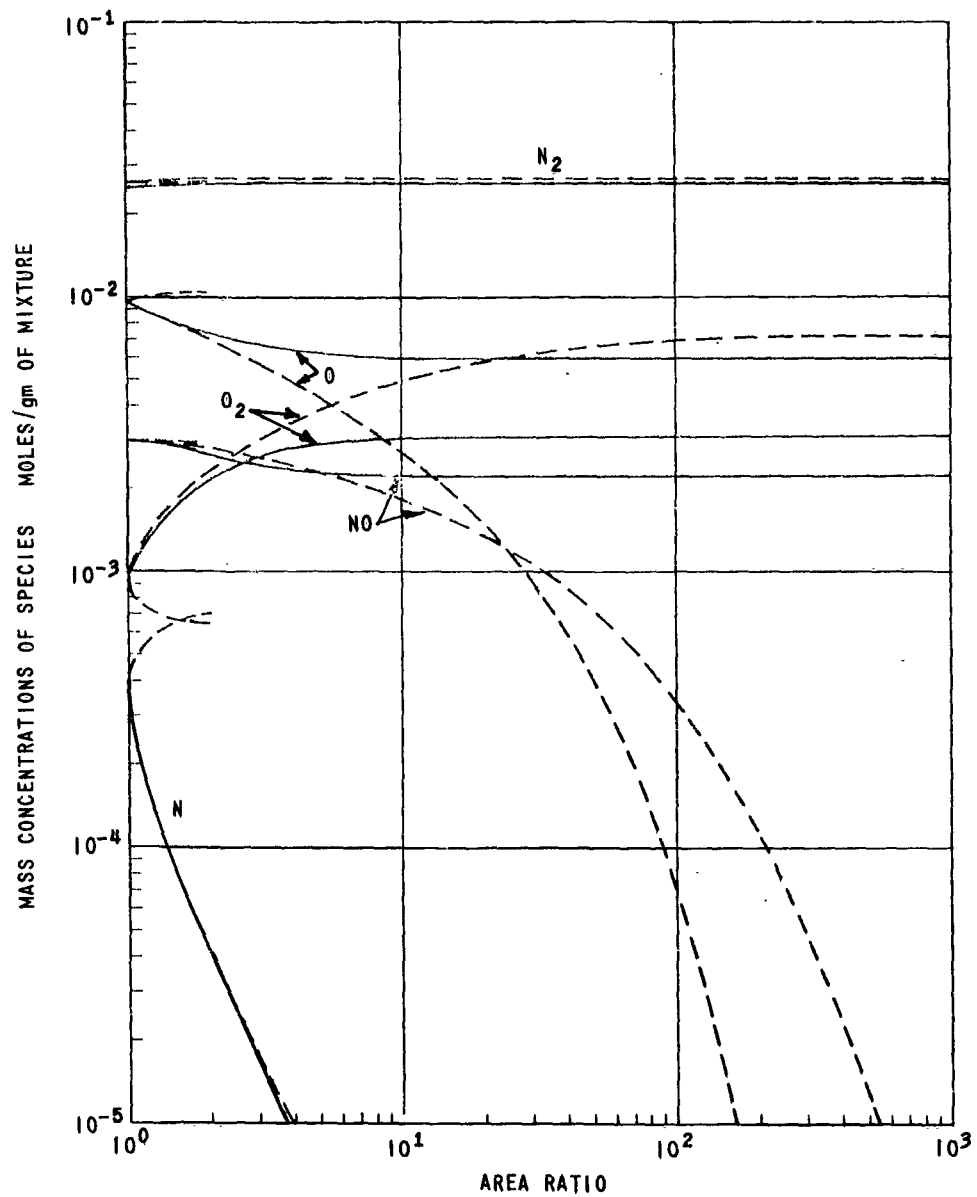


FIG.5 SPECIES DISTRIBUTIONS FOR AIRFLOW IN A HYPERSONIC NOZZLE

$$T_0 = 6000^\circ K \quad P_0 = 100 \text{ ATM} \quad l = 1 \text{ cm}$$

———— FINITE RATE NONEQUILIBRIUM  
 - - - - - INFINITE RATE EQUILIBRIUM

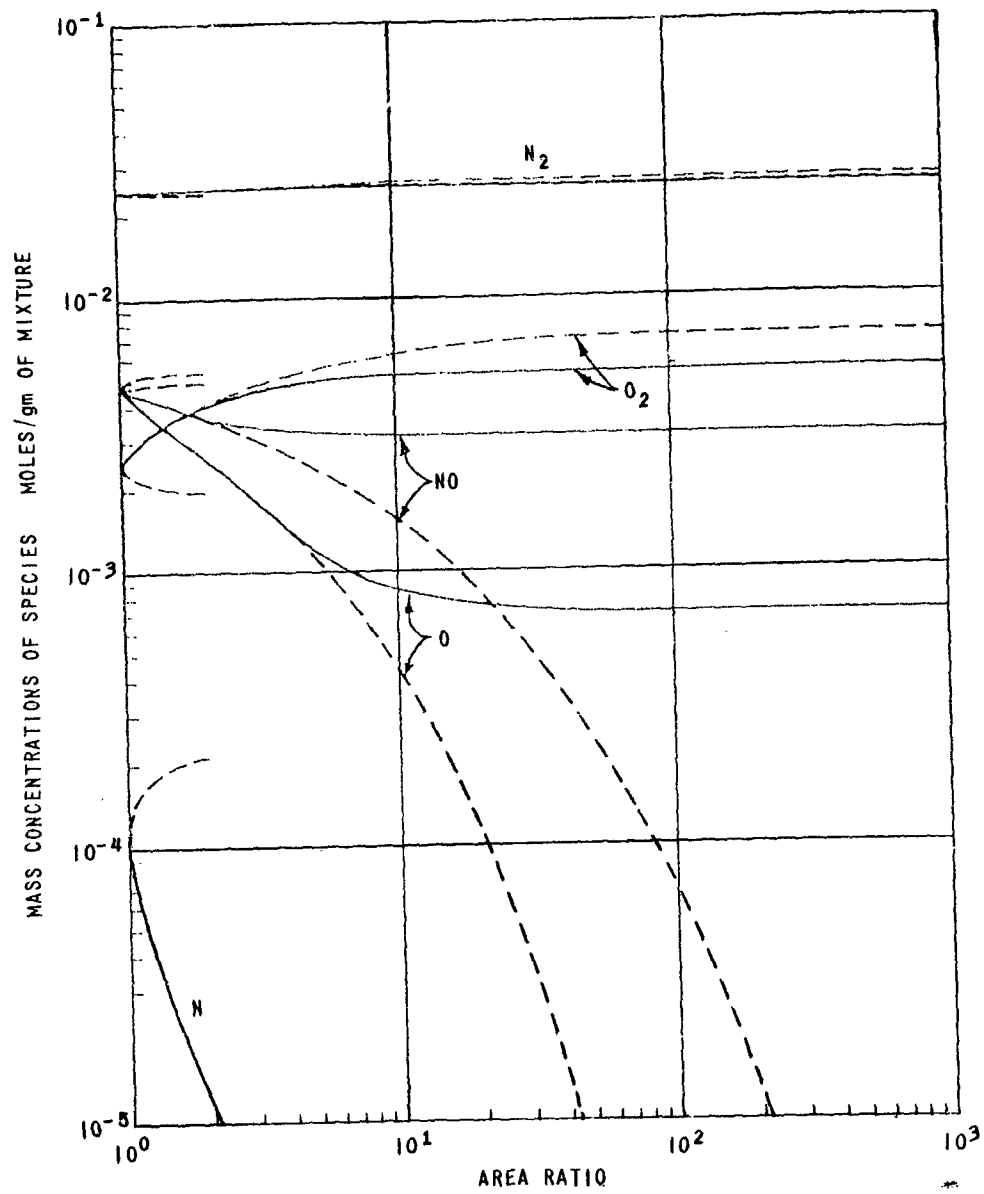


FIG. 6 SPECIES DISTRIBUTIONS FOR AIRFLOW IN A HYPERSONIC NOZZLE

$$T_0 = 6000^\circ K, P_0 = 1000 \text{ ATM } d = 1 \text{ cm}$$

———— FINITE RATE NONEQUILIBRIUM  
 - - - - - INFINITE RATE EQUILIBRIUM

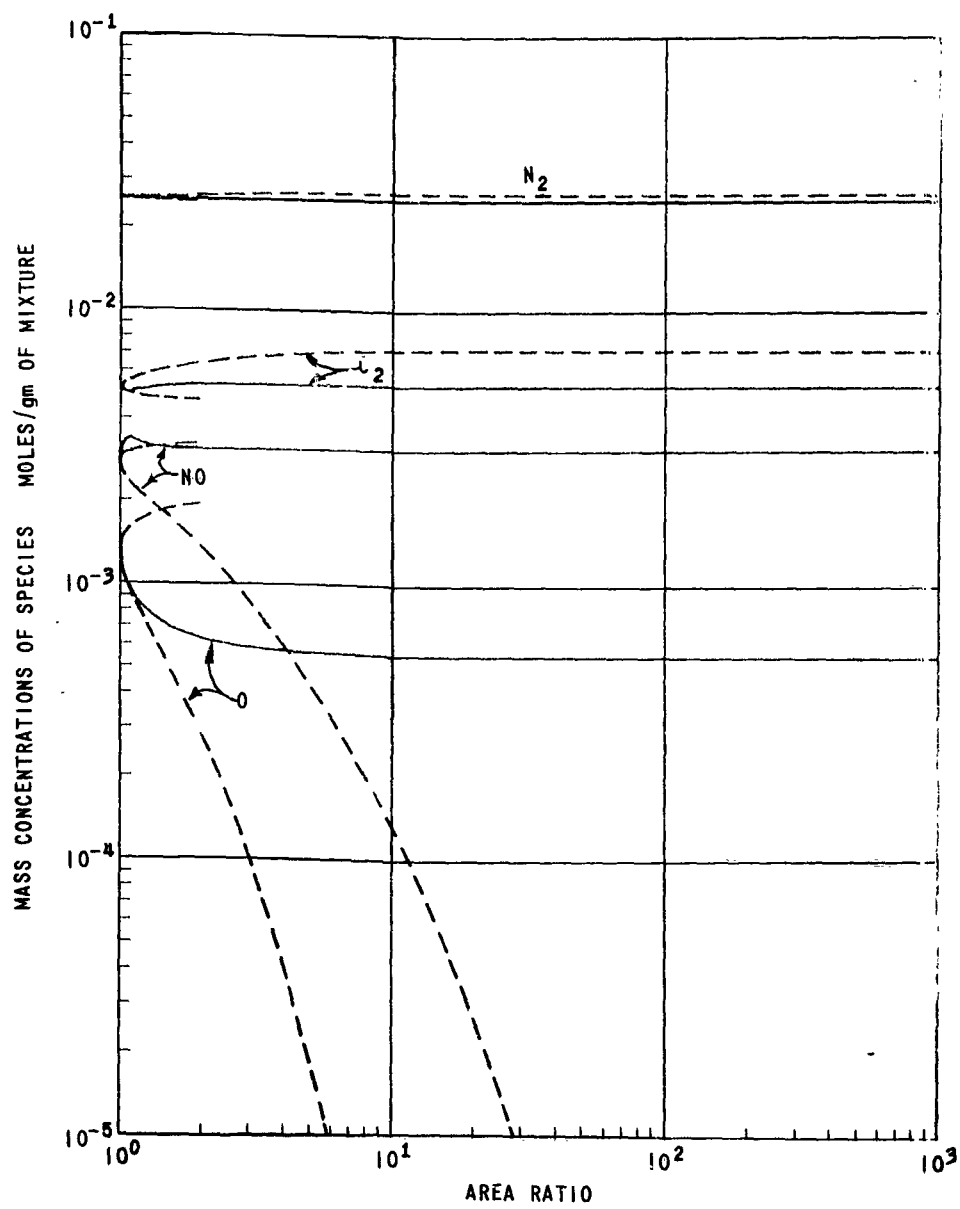


FIG.7 SPECIES DISTRIBUTIONS FOR AIRFLOW IN A HYPERSONIC NOZZLE

$$T_0 = 4000^\circ K, P_0 = 100 \text{ ATM } L = 1 \text{ cm}$$

———— FINITE RATE NONEQUILIBRIUM  
 - - - - - INFINITE RATE EQUILIBRIUM